1990

Simulation of Free Radical Reactions in Biology and Medicine: A New Two-Compartment Kinetic Model of Intracellular Lipid Peroxidation

Charles F. Babbs
Purdue University, babbs@purdue.edu

Melissa Gale Steiner

SIMULATION OF FREE RADICAL REACTIONS IN BIOLOGY AND MEDICINE: A NEW TWO-COMPARTMENT KINETIC MODEL OF INTRACELLULAR LIPID PEROXIDATION

CHARLES F. BABBS and MELISSA GALE STEINER

Biomedical Engineering Center, Purdue University, West Lafayette, Indiana, USA.

Abstract -- To explore mechanisms of free radical reactions leading to intracellular lipid peroxidation in living systems, we developed a computational model of up to 109 simultaneous enzymatic and free radical reactions thought to be involved in the initiation, propagation, and termination of membrane lipid peroxidation. Rate constants for the various reactions were obtained from the published literature. The simulation model included a lipid membrane compartment and an aqueous cytosolic compartment, between which various chemical species were partitioned. Lipid peroxidation was initiated by the iron-catalyzed, superoxide-driven Fenton reaction. A "C"-language computer program implemented numerical solution of the steady-state rate equations for concentrations of nine relevant free radicals. The rate equations were integrated by a modified Euler technique to describe the evolution with time of simulated concentrations of hydrogen peroxide, ferric and ferrous iron, unsaturated lipid, lipid hydroperoxides, superoxide anion, and biological antioxidants, including SOD and catalase. Initial results led to significant insights regarding mechanisms of membrane lipid peroxidation:

1. segregation and concentration of lipids within membrane compartments promotes chain propagation;
2. in the absence of antioxidants computed concentrations of lipid hydroperoxides increase linearly about 40 µM/min during oxidative stress;
3. lipid peroxidation is critically dependent upon oxygen concentration and the modeled dependence is similar to the experimental function;
4. lipid peroxidation is rapidly quenched by the presence of Vitamin E-like antioxidants, SOD, and catalase;
5. only small (l to 50 µM) amounts of "free" iron are required for initiation of lipid peroxidation;
6. substantial lipid peroxidation occurs only when cellular defense mechanisms have been weakened or overcome by prolonged oxidative stress, hence understanding of the balance between free radical generation and antioxidant defense systems is critical to the understanding and control of free radical reactions in biology and medicine.
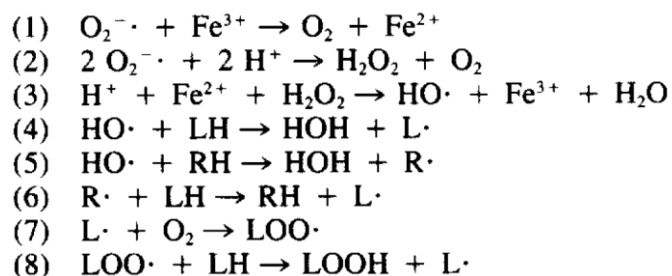
INTRODUCTION

Free radicals are currently thought to be significant agents of tissue injury in a large number of disease states afflicting man and animals.[1-6] Owing to their high reactivity, most free radicals postulated to attack biologic substrates must exist in vivo in extremely low instantaneous concentrations. The measurement of highly reactive free radicals such as the hydroxyl radical (HO•) therefore represents a formidable technical challenge, which is only beginning to be met in quantitatively meaningful ways.[7-10] At present, there remains an open question as to whether free radical generation within living cells is inconsequential or pathophysiological, that is, whether free radicals are easily detoxified byproducts, produced in relatively small numbers, or whether under some circumstances cells are capable of making free radicals in sufficient numbers to cause their own self-destruction.

Computer modeling offers one approach to investigation of this question. The fundamental kinetics of the most quoted reactions postulated to cause radical mediated cell injury are well known from the published literature. The process of calculating the extremely small, instantaneous free radical concentrations according to the "steady-state" hypothesis is well established,[11-13] and can be done in a computationally intensive, but straightforward manner by numerical methods. Numerical integration of many simultaneous differential equations is also a conceptually simple, but tedious task, well suited to modern, high speed computers. Previously computational models have proved valuable in elucidation of free radical reactions occurring in flame chemistry and in photochemical smog, and recently in ozone depletion in the high atmosphere.[14-17] A recent report of Tappel and coworkers has pointed out the advantages of simulation modeling of oxidative reactions in biology.[18]

Following this tradition, the authors have developed a library of conceptually simple, modular, "C"-language computer code during the past 3 years to solve the steady state rate equations for free radical chain reactions proposed to occur during oxidative stress in biological systems. This paper describes the creation of the model, and initial results and insights derived therefrom. The particular form of oxygen radical injury to tissue that has most interested us is known as reoxygenation or reperfusion injury, in which a burst of oxygen radicals is thought to be generated when oxygen is suddenly restored to previously hypoxic tissues. This type of rapid reoxygenation occurs, for example, in resuscitation after cardiac arrest or in the treatment of acute coronary artery occlusion following lysis of a blood clot that obstructed the artery. A chemical explanation for reoxygenation injury has been evolving, and has been the subject of several reviews.[6, 19, 20] A synthesis of the most quoted chemical mechanisms includes the reactions listed in Table 1.

2

Table 1. Putative Initiation and Chain Propagation Reactions in
Reperfusion Injury Mediated by Oxygen Radicals

$$(1) \quad O_2^- \cdot + Fe^{3+} \rightarrow O_2 + Fe^{2+}$$
$$(2) \quad 2\,O_2^- \cdot + 2\,H^+ \rightarrow H_2O_2 + O_2$$
$$(3) \quad H^+ + Fe^{2+} + H_2O_2 \rightarrow HO\cdot + Fe^{3+} + H_2O$$
$$(4) \quad HO\cdot + LH \rightarrow HOH + L\cdot$$
$$(5) \quad HO\cdot + RH \rightarrow HOH + R\cdot$$
$$(6) \quad R\cdot + LH \rightarrow RH + L\cdot$$
$$(7) \quad L\cdot + O_2 \rightarrow LOO\cdot$$
$$(8) \quad LOO\cdot + LH \rightarrow LOOH + L\cdot$$

The putative pathological chemistry begins with the sequence of reactions (1-3), known collectively as the superoxide-driven Fenton reaction. Superoxide ions ($O_2^-\bullet$) are thought to be generated by the action of xanthine oxidase upon accumulated xanthine or hypoxanthine substrates,[19] as well as by the actions of mitochondria and activated leukocytes. Both xanthine oxidase and hypoxanthine have been shown to be elevated in postischemic tissues,[19, 21, 22] owing both to the conversion of xanthine dehydrogenase to xanthine oxidase and to the accumulation of hypoxanthine in ischemic tissues. The hydroxyl radicals ($HO\bullet$) formed in reaction (3) might then attack cellular proteins (RH) and lipids (LH) directly or via intermediate radicals ($R\bullet$) of longer half-life (reactions 4-6). The abstraction of hydrogen ions from membrane phospholipids by radicals (reactions 4, 6, and 8) occurs most readily at sites of two or more double bonds.[23] The lipid alkyl radicals ($L\bullet$) can then react with molecular oxygen (7), even at the low concentrations present during incomplete ischemia[24] and especially during reperfusion when oxygen is abundant, followed by slow chain propagation in the organized structure of membranes (7, 8). The latter is a self-propagating sequence for lipid peroxidation.

In the present investigation we chose to focus on the generation of LOOH as the presumed principal product of pathological free radical chemistry, because these compounds have been most extensively studied as end products of oxidative tissue injury.[23, 25-28] In particular, lipid hydroperoxides may biophysically alter the character of the cell membrane[25] rendering it leaky to calcium ions and intracellular proteins. Lipid hydroperoxides may also break down into toxic products such as 8-hydroxynonenal[29] or oxidized arachadonic acid derivatives.[30]

To determine if pathological chemistry similar to that just described is a kinetically reasonable route to the production of membrane lipid hydroperoxides in cells during reoxygenation after ischemia, one of us (CFB) began to develop a computer model of lipid peroxidation in 1985, which has slowly evolved in its sophistication. This paper describes the model and the initial mechanistic insights it has provided.

COMPUTATIONAL METHODS

General features

The software employed in the present research performs steady-state solution and then numerical integration of the simultaneous kinetic equations describing the superoxide driven Fenton reaction, lipid peroxidation reactions, and subsequent secondary radical and chain termination reactions. The output includes concentrations of the various radical and nonradical species at specified sampling times, calculated as functions of all the other concentrations. A "C"-language software library first implements a modified Gauss-Seidel technique to solve the simultaneous steady-state equations, $dr_i/dt = 0$, for the concentrations of reactive intermediate radicals, r_i, including HO•, L•, LO•, LOO•, R•, RO•, ROO•, A•, and GS•, where L is an oxidizable lipid, R is an oxidizable nonlipid, A is a vitamin E-like membrane antioxidant, and GSH is a glutathione-like cytosolic antioxidant. Superoxide is treated numerically as a nonradical species to reflect its relatively low reactivity, and to allow convenient manipulation of its concentration. In the second phase of computation a simple Euler method is applied to integrate the various concentration versus time curves for each nonradical species. Radical concentrations are recalculated from the steady state equations at specified intervals much longer than dt, in keeping with the steady state assumption.

Steady state equations

The first stage of the hybrid numerical method employed in the present model requires the solution the classical steady-state equations, $dr_i/dt = 0$, to obtain the concentrations of the highly reactive free radicals, r_i, in the system. The steady state equations are excellent approximations, based upon the stationary state or steady-state assumption for non-exploding systems of coupled free radical reactions,[12, 13] which states that the instantaneous concentrations of highly reactive intermediates are extremely small compared to the concentrations of other species in the system, and in turn the absolute values of the time derivatives of reactive free radical concentrations are approximately equal to zero. This assumption must hold in a more-or-less steadily progressing reaction involving free radicals, since if the population of reactive intermediate radicals were increasing, the rate of product formation would accelerate in an explosive manner, and if the population of radicals were decreasing, the rate of product formation would be rapidly quenched. Hence, for a system of rate equations describing the formation and disappearance of N free radicals, a set of N stationary state equations and N unknown radical concentrations can be defined, as described by Gimblett[12] and Emanuel.[13]

In the software developed for the present application, seed values for the unknowns are taken as first estimates for radical concentrations, and the estimates are continually improved by a modified Gauss-Seidel iteration. Typically, seed values are based on the results of brief (10 sec) trial simulations, and previous experience with similar models. The stationary state equation for the most reactive free radical (HO•) is evaluated first, the stationary state equation for the next most reactive radical second, and so forth, in the order HO•, L•, LO•, LOO•, R•, RO•, ROO•, A•, and GS•. This approach creates a coefficient matrix for the complete set of equations that is

very nearly triangular, and hence quite efficiently solved by the modified Gauss-Seidel approach.[31]

We use the term "modified Gauss-Seidel," because some of the stationary state equations contained squared terms, derived from radical-radical termination reactions. Hence, the set of equations to be solved is not necessarily linear. To permit convergence of the iterative method in simulations with prominent radical chain termination reactions, it was necessary to introduce a damping factor, α, with value between zero and unity, and to replace the new estimate, r_i^{n+1} of radical species, i, at time step n + 1, with $\alpha r_i^{n+1} + (1 - \alpha) r_i^n$. When $\alpha = 1$, the method is identical to the usual Gauss-Seidel iteration for linear equations. When termination reactions are prominent, a suitable choice of $\alpha < 1$ (e.g., $\alpha = 0.03$) allows convergence of the iteration to solve for the small, instantaneous concentrations of free radical species, despite the presence of quadratic terms.

Numerical integration

The second stage of the hybrid numerical method employs a simple Euler method for numerical integration of the rate equations in order to compute the evolution of reactant concentrations over time.[31] The Euler program module calculates concentrations of the various species after successive small time steps, dt, as functions of all the other concentrations and the rate constants. For all reactions A + B $\rightarrow$ C + D, nonradical reactant concentrations at the end of the next time increment are estimated as the current concentration plus the incremental change, $-dA = k[A][B]dt$.

This process is repeated many times to track changes in reactant concentrations for a predetermined number of time steps. In the present study, sufficiently small time steps for integration were selected such that halving or doubling the time step did not affect the results. Central to the integration of non-enzymatic kinetic equations is a subroutine to compute the concentration changes during a differential time step, dt, produced by a family of competing bimolecular reactions of the form

$$A + B_1 \longrightarrow C_1 + D_1,$$

$$A + B_2 \longrightarrow C_2 + D_2,$$

$$A + B_3 \longrightarrow C_3 + D_3,$$
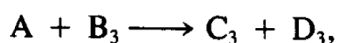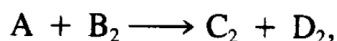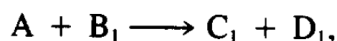
$$\text{etc.,}$$

for which it is assumed that species A is most reactive (usually a radical). In the case that the consumption of A is rate-limiting, the distribution of products is determined according to competition kinetics, as described by Spinks.[32] The kinetic behavior of the enzyme xanthine oxidase is modeled as a ping-pong/bi-bi mechanism, as described by Walsh.[33] The enzymatic reactions of superoxide dismutase and catalase are simulated by application of pseudo-first order rate constants for the reaction of enzyme with substrate, $k' = 2 \times 10^9 \ M^{-1}sec^{-1}$ for SOD[34] and

5

k' = 4×10^7 M^{-1}sec^{-1} for catalase.[35] The kinetic model was validated repeatedly during the course of its development by comparison of computed solutions with known analytical solutions for simple test cases.

Specification of relevant reactions

Cumulative lipid hydroperoxide production by free radical mediated oxidation of unsaturated lipids was computed assuming the simultaneous occurrence of 32 relevant enzymatic and free radical reactions, described by rate constants obtained from the published literature (Table 2). Degradation of lipid hydroperoxide, once it had been formed, by reactions such as Fe^{2+} + LOOH → Fe^{3+} + OH$^-$ + LO•, was deliberately excluded to focus on total or cumulative formation of abnormally oxidized lipids. The kinetic model containing the set of 32 kinetic equations was derived from a much larger model including over 109 reactions described in the published literature (available from the authors on request) that could conceivably have played a role in this or similar systems. The list of equations ultimately included in the present model was obtained from the complete list by omitting obviously irrelevant ones, and by eliminating reactions which formed zero or negligible product (less than 0.1 µM) during the course of representative test simulations.

Table 2. Rate Constants in the Model

Reaction	Rate	Constant
$H_2O_2 + Fe^{2+} \rightarrow Fe^{3+} + HO\cdot$	$9e+5$	$k[0]^{58}$
$HO\cdot + Fe^{2+} \rightarrow Fe^{3+} + OH^-$	$3e+8$	$k[1]^{59}$
$HO\cdot + LH \rightarrow L\cdot + H_2O$	$1e+9$	$k[3]^{11}$
$O_2^-\cdot + Fe^{3+} \rightarrow Fe^{2+} + O_2$	$1e+6$	$k[4]^{58}$
$L\cdot + O_2 \rightarrow LOO\cdot$	$9e+6$	$k[5]^{49}$
$LOO\cdot + LH \rightarrow LOOH + L\cdot$	31	$k[6]^{60}$
$H_2O_2 \rightarrow H_2O + 1/2\ O_2$ (catalase)	$1.5e+7$	$k[13]^{61}$
$O_2^-\cdot + O_2^-\cdot + 2\ H^+ \rightarrow H_2O_2 + O_2$	$6e+5$	$k[15]^{62}$
$LOO\cdot + AH \rightarrow LOOH + A\cdot$	$1e+5$	$k[16]^{49}$
$HO\cdot + RH \rightarrow R\cdot + H_2O$	$1e+8$	$k[28]^{11}$
$HO\cdot + AH \rightarrow A\cdot + H_2O$	$1e+10$	$k[30]^{63}$
$L\cdot + AH \rightarrow L'H + A\cdot$	$4.5e+6$	$k[31]^{64}$
$HO\cdot + O_2^-\cdot \rightarrow O_2 + OH^-$	$1e+10$	$k[32]^{63}$
$R\cdot + O_2 \rightarrow ROO\cdot$	$3e+8$	$k[37]^{65}$
$ROO\cdot + Fe^{2+} + H_2O \rightarrow Fe^{3+} + OH^- + ROOH$	$4.5e+6$	$k[39]^{64}$
$O_2^-\cdot + ROO\cdot + H_2O \rightarrow ROOH + OH^- + O_2$	$1e+8$	$k[50]^{66}$
$L\cdot + L\cdot \rightarrow L-L$	$2e+8$	$k[60]^{67}$
$L\cdot + LOO\cdot \rightarrow LOOL$	$5e+7$	$k[61]^{49}$
$L\cdot + A\cdot \rightarrow L-A$	$4e+5$	$k[66]^{49,67}$
$LOO\cdot + LOO\cdot \rightarrow LOOL + O_2$	$3e+7$	$k[67]^{68}$
$LOO\cdot + A\cdot \rightarrow LOOA$	$1e+5$	$k[72]^{49}$
$A\cdot + A\cdot \rightarrow A-A$	$1e+3$	$k[87]^{49,67}$
$2\ O_2^-\cdot + SOD + 2\ H^+ \rightarrow H_2O_2 + O_2$	$1e+6$	$k[88]^{69}$
$xanthine + O_2 \rightarrow uric\ acid + O_2^-\cdot$	15	$k[89]^{70}$
$hypoxanthine + O_2 \rightarrow xanthine + O_2^-\cdot$	15	$k[90]^{70}$
$Fe^{2+} + O_2 \rightarrow Fe^{3+} + O_2^-\cdot$	$6e+2$	$k[92]^{71}$
$R\cdot + Fe^{2+} \rightarrow Fe^{3+} + R'H$	$1e+7$	$k[101]^{11}$
$HO\cdot + GSH \rightarrow GS\cdot + H_2O$	$9e+9$	$k[102]^{32}$
$R\cdot + GSH \rightarrow GS\cdot + RH'$	$1e+9$	$k[104]^{32}$
$ROO\cdot + GSH \rightarrow ROOH + GS\cdot$	$1e+4$	$k[105]^{60}$
$O_2^-\cdot + GS\cdot + H_2O \rightarrow GSH + O_2 + OH^-$	$7e+5$	$k[108]^{34}$
$GS\cdot + GS\cdot \rightarrow GSSG$	$2e+9$	$k[109]^{72}$

*The notation ae + b is equivalent to a x 10^b.

The software was capable of solving any number of simultaneous equations from 2 to 109 without modification of the code. The program was so configured that if input rate constants were read as zero, the corresponding computations were simply not performed (i.e., arrays of pointers indicating reactions to be included in the simulation were resorted to exclude reactions with zero rate constants). This feature maximized the generality and convenience of the software library and minimized execution time, for any selected simulation.

Two compartment extension of the model

A preponderance of literature on the significance of free radical reactions in biology and medicine focuses on cell membrane lipid peroxidation as the major toxic consequence of free

radical generation in biological systems. In vivo cellular lipids vulnerable to peroxidation are not freely soluble, but rather arranged in phospholipid bi-layer membranes or confined to lipid droplets. Accordingly, we sought to adapt the original model of a homogeneous, one-phase solution to that of a two-phase system, incorporating both aqueous and membrane lipid compartments. In this model we define the total volume, V_T as the sum of the volume of the aqeuous compartment, V_1 and the volume of the lipid compartment, V_2. These and other parameters relevant to compartmentalization are presented in Table 3.

Table 3. Variables of the Two-Compartment Model

V_1	aqueous volume
V_2	lipid volume
V_T	total volume
$r = \dfrac{V_1 + V_2}{V_2}$	compartment volume ratio (>1)
$q_A = \dfrac{[A]_2}{[A]_1}$	lipid/water partition coefficient for reactant, A
$q_B = \dfrac{[B]_2}{[B]_1}$	lipid/water partition coefficient for reactant, B
c_1	reactant concentration in compartment 1
c_2	reactant concentration in compartment 2
$\bar{c}$	volume averaged, mean concentration in both compartments

The fundamental strategy for creation of the two phase model is to define an equivalent one-phase model having reactant concentrations equal to the mean, volume-averaged reactant concentrations of the two phase system and also having reaction rate constants adjusted to account for the effects of phase separation. The conversion from compartmental concentrations to mean concentration is entirely straightforward, namely

$$c_1 = \frac{r}{q + r - 1}\,\bar{c} \quad \text{and} \quad c_2 = \frac{qr}{q + r - 1}\,\bar{c}, \quad (1)$$

where, partition coefficient, $q = c_2/c_1$. Using equations (1) it is possible, whenever desired, to transform between specific compartmental concentrations, c_1 and c_2, and the mean concentration, $\bar{c}$ for any reactant. This approach assumes equilibrium between the phases, as described by partition coefficient, q.

The strategy for determining the rate constants of a one phase model that account for the effects of phase separation upon the kinetics of the two phase system is based upon the following insight. If one assumes that the reaction

$$A + B \xrightarrow{k} C + D \qquad (2)$$
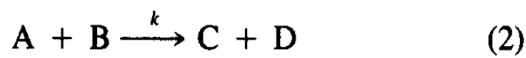
proceeds with a similar rate constant, k, such that $-d[A]/dt = k[A][B]$, in both the lipid and the aqueous phase, then the mean, volume-averaged, reaction rate for the two-phase system is a computable function of the rate constant, k, and the lipid/water partition coefficients of the reactants, q_A and q_B. In particular, as shown formally in the Appendix,

$$\frac{-d[A]}{dt} = \frac{(q_A q_B + r - 1)r}{(q_A + r - 1)(q_B + r - 1)} k[A][B]$$

$$= k_{eq}[A][B]. \quad (3)$$

From equation (3) it is clear that the mean, volume averaged rate of reaction in the two compartment model is directly proportional to the reaction rate, $k[A][B]$, that would have occurred if the reactants had been uniformly distributed in solution in a one-compartment model at their mean concentrations. The constant of proportionality, equal to the coefficient of $k[A][B]$ in equation (3), is a simply computable function of the lipid/water partition coefficients for reactants A and B and the fractional volume of the lipid compartment, $1/r$. In turn, one can define an equivalent rate constant, k_{eq}, for a simple one-compartment model, in which the evolution of mean concentration changes over time is the same as in the two-compartment model. The individual compartment concentrations can then be found, using equations (1).

In this way it is possible to solve a two-compartment problem with one compartment software, after a simple transformation of the compartmental concentrations to mean concentration, together with simple transformation of the matrix of rate constants, [k], to the matrix of rate constants, [k_{eq}]. The required transformations can be appreciated intuitively and reasonably approximated in many cases. Consider, for example the case of the chain propagation reaction for lipid peroxidation,

$$LOO\cdot + LH \xrightarrow{k_6} LOOH + L\cdot,$$
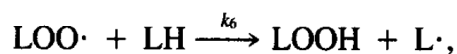
in a two-phase model containing 10% lipid, that is, $r = 10$. This reaction takes place in the lipid phase only.

Let [LOO·] and [LH] represent the mean, volume averaged concentrations; $[LOO\cdot]_1 = [LH]_1 = 0$ represent the zero concentrations in the aqueous phase; and $[LOO\cdot]_2$ and $[LH]_2$ represent the concentrations in the lipid phase, which are 10 times the mean concentrations. The rate of reaction in the lipid phase will therefore be

9

$$-d[\text{LH}]_2/dt \; = \; k[\text{LOO·}]_2[\text{LH}]_2 \; = \; 100k[\text{LOO·}][\text{LH}],$$

or more generally

$$-d[\text{LH}]_2/dt \; = \; r^2k[\text{LOO·}][\text{LH}].$$

The change in mean concentration, however will be 1/10th as great as that in the lipid compartment, or generally

$$-d[\text{LH}]/dt \; = \; rk[\text{LOO·}][\text{LH}].$$

In this example, then, the effect of phase separation in the two-phase system is to increase the apparent rate constant for chain propagation by a factor of $r = 10$. Hence, to model the kinetics of this reaction in a two phase system, it is possible to run a one-phase model with mean reactant concentrations equal to those of the two-phase system and with a transformed rate constant, $k_{eq} = rk$, 10 times the original value. In this example the reaction is accelerated, because reactants are concentrated in the lipid phase. In a similar manner, and also by application of equation (3), it is possible to show that for the limiting cases of various combinations of highly water soluble reactants ($q = 0$) and highly lipid soluble reactants ($q = \infty$) the transformed rate constants describing the kinetics of the two-phase system are as shown in Table 4.

Table 4. Rate Constant Transformations for Two-Phase Model

$$A + B \xrightarrow{k} C + D$$

q_A	q_B	k_{eq}
∞	0	0
0	∞	0
1	1	k
0	0	$rk/(r-1)$
∞	∞	rk
∞	1	k
1	∞	k
0	1	k
1	0	k

Note that if one of two reactants is confined to one compartment and the second reactant to another compartment, the reaction rate will be zero. If both reactants are confined to a single compartment, a concentration effect is seen. In the remaining cases the equivalent rate constant for the two-phase system is the same as for the one-phase system.

Initial conditions

In the current simulations we sought to capture the essence of biological lipid peroxidation in a two-phase model by assuming that reactants were either entirely lipid soluble (q = ∞), entirely water soluble (q = 0), or equally soluble in the two phases (q = 1), according to the specifications listed in Table 5. In this case, the simplified transformation of rate constants amounted to multiplication of k values for lipid-lipid compartment reactions by r (taken as 40 for a typical cell)[36] or multiplication of k values by zero for phase-segregated reactants.

Table 5. Assumed Compartmentalization of Species and Their Initial **Mean** Concentrations (μM)

Confined to Aqueous Compartment Only ($q = 0$)	Confined to Lipid Compartment Only ($q = \infty$)	Distributed to Both Compartments ($q = 1$)
Radicals		
R· (~0)	L· (~0)	HO· (~0)
ROO· (~0)	LOO· (~0)	
RO· (~0)	LO· (~0)	
GS· (~0)	A· (~0)	
Nonradicals		
RH (100,000)	LH (50,000)	H_2O_2 (0)
ROOH (0)	LOOH (0)	O_2 (50)
O_2^-· (0)	LX (0)	
HX (1000)	AH (50)	
X (0)		
XO (0.15)		
SOD (10)		
CAT (10)		
UA (0)		
GSH (5000)		
Fe^{2+} (100)		
Fe^{3+} (0)		

Because our initial models were intended to represent the first few minutes of reoxygenation after tissue ischemia, iron at time zero was assumed to be in the reduced, ferrous state, which would be expected under anaerobic conditions. Hypoxanthine concentrations were selected on the basis of reports of Jennings,[37] Buhl,[38] and Ratych et al.[39] of hypoxanthine concentration in postischemic heart and kidney tissue. Xanthine oxidase activity was based upon that reported by DellaCorte for the rat (80 mUnits/g).[40]

Our initial computational models, variations of which were also studied, contained 50 mM polyunsaturated fatty acids susceptible to lipid peroxidation, and 1 mM hypoxanthine, and 0.15 μM xanthine oxidase. This amount of hypoxanthine was sufficient to metabolize 1 mM

hypoxanthine to uric acid in about 15 min. The standard model included 100 µM iron modeled as the EDTA-chelate, sufficient to induce lipid peroxidation in vitro[23, 41] and roughly equivalent in activity to the low molecular weight chelate iron in postischemic dog brain and heart.[42, 43] EDTA-chelated iron is commonly used in laboratory models of lipid peroxidation. The actual in vivo iron chelators that may be operative in free radical-mediated injury are not known, but may include either ADP[44] or citrate,[45] which are about one-third as effective as EDTA-chelated iron. In some simulations, the presence of low, normal, and high levels of endogenous antioxidants (such as Vitamin E) was modeled. Oxygen concentration was modeled over a range from zero to 1000 µM, taking as a reference the value of 200 µM for the dissolved oxygen concentration in air saturated water[46] and a corresponding conversion of 1 µM = 0.70 mmHg. The standard model of nonischemic tissue contained 50 µM oxygen.

Using the foregoing computational strategy, we explored the production of LOOH in a two-phase model of biological cells containing varying amounts of iron, oxygen, Vitamin-E-like antioxidants, superoxide dismutase, and catalase. Simulations were run on either a Sun 3/60 work station or a Sun 4 mini-computer, each operating under UNIX and capable respectively of approximately 1×10^6 and 8×10^6 double-precision floating point operations per second. Typical execution times ranged from 2 to 60 min. Outputs of computations included concentrations of all radical and nonradical species as functions of time, checks and balances to ensure that steady state criteria for reactive radical species were met, and chemical "fluxes" through each simulated reaction (i.e., the total number of molecules of species A consumed in reaction, A + B → products, for the duration of the simulation).

RESULTS

Compartmentalization

Figure 1 illustrates the effects upon lipid peroxidation of compartmentalization of lipids within membranes. Simulated net accumulation of lipid hydroperoxides (LOOH) is plotted as a function of time under favorable conditions for LOOH formation (no superoxide dismutase, catalase, or membrane antioxidant). We refer to this as an "undefended model," because antiradical defense mechanisms are absent. The lower curve (1C) represents LOOH accumulation in an undefended one-compartment model, in which all species are treated as if in dilute solution.
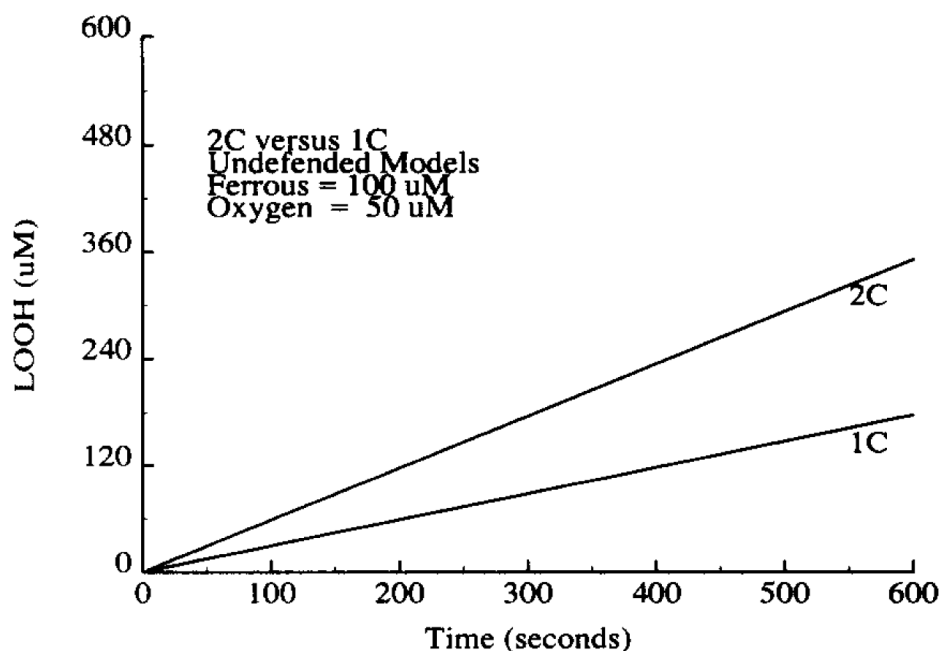
Fig. 1. Effects upon lipid peroxidation of compartmentalization lipids within membranes. Lower curve (1C) describes the one compartment model; upper curve (2C) describes the two compartment model. Compartmentalization of lipids greatly increases LOOH formation.

The upper curve (2C) represents LOOH accumulation in an undefended two-compartment model, in which peroxidizable lipid species are treated as if confined in a membrane-like compartment of total volume 1/40th that of bulk tissue. Membrane compartmentalization clearly enhances the amount of lipid peroxidation in this model system. Analysis of specific reaction fluxes reveals that chain propagation ($LOO\bullet + LH \rightarrow LOOH + L\bullet$), in particular, is greatly enhanced (0.25 to 351.91 µM after 10 min) in the compartmentalized model, owing to the higher local concentration of lipid and lipid radicals within the membrane. In the one compartment model, chain length for propagation of lipid peroxidation (i.e., the steady state rate of total LOOH formation divided by steady state rate of $L\bullet$ formation by reaction 3) was only 0.0014, while in the two-compartment model with otherwise identical initial conditions, chain length was 1.71. Thus, even though chain propagation is relatively slow ($k = 32$ $M^{-1}sec^{-1}$), the concentration of lipids within the membranes can make chain propagation significant. Since compartmentalization of lipids is certainly expected in vivo, all further simulations were performed with the assumptions of the two-compartment model, as defined in Tables 4 and 5.

Compact format for lipid peroxidation data

To characterize lipid peroxidation in the two-compartment simulation model, we noted that the rate of LOOH formation is approximately linear under steady state conditions, as long as superoxide is being produced. Analysis of preliminary results under a variety of conditions showed that the final value of LOOH accumulated at 10 min is a convenient measure of the overall rate of lipid peroxidation. A 10-min period corresponds roughly to the duration of the respiratory burst of leukocytes[47] and to the interval during which hypoxanthine concentration remains elevated in postischemic cardiac muscle[37] as a potential source of excessive superoxide formation.

Sensitivity analysis

To assess the sensitivity of final lipid hydroperoxide concentration to potential errors in assumed rate constants, we performed a sensitivity analysis, in which the fractional change in LOOH concentration during a test simulation was compared to the fractional change in each rate constant for representative test simulations.

In particular, we adopted the method of Dodge[16], in which the rate equations were first integrated with all the constants at their "standard" values (Table 2) to obtain the concentration-time profile for LOOH. Then one of the rate constants was doubled, that is, increased by 100%, while all the other rate constants were held fixed. The model was re-solved with these new settings, and the concentration-time curve for LOOH re-plotted. The fractional change in the area under the LOOH versus time curve (absolute value in percent) was divided by the fractional change in the selected rate constant (100%) to obtain the sensitivity ratio for each rate constant. To reduce computation time to a reasonable amount, a coarser time resolution *(*dt = 0.01 sec) for numerical integration and a shorter simulation time (duration = 10 sec) were used for the 64 separate simulations required in the sensitivity analysis.

The results of are presented in Fig. 2, in which the sensitivity ratio in a standard undefended model is plotted as a function of the discrete rate constant ID numbers in Table 2. Nine rate constants showed a sensitivity ratio greater than 0.1, indicating that a 100% change in assumed rate constant caused a greater than 10% change in eventual lipid peroxidation. These more critical reactions included reactions 0, 3, 5, 6, 60, 61, 67, 89, and 102, which can be arranged in a rational sequence as shown in Table 6. The general scheme of the critical reactions, as revealed by the sensitivity analysis, is quite similar to that in prior reports of free radical-mediated lipid peroxidation (Table 1). These rate constants are relatively well established in the published literature, in most cases on the basis of several sources.[48]
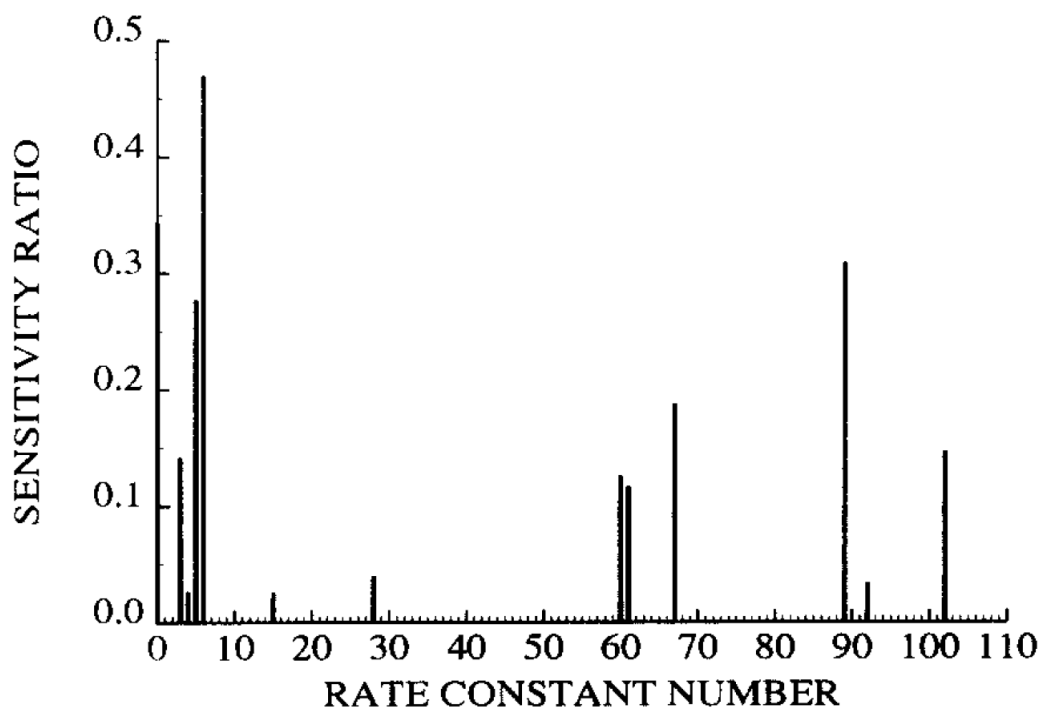

Fig. 2. Sensitivity analysis. Rate constants are identified by number as in Table 2. The sensitivity ratio is the relative change in LOOH formation divided by the relative change in a single specified rate constant. A large sensitivity ratio indicates that a change in the specified rate constant has a meaningful effect on the rate of lipid peroxidation.

Table 6. Key Reactions Identified by Sensitivity Analysis

Reaction	Rate Constant 1/(mol-s) ± SD	Rate Constant ID and References
Initiation		
xanthine + $O_2 \rightarrow$ uric acid + $O_2^-\cdot$	15.2 ± 1.4	$k[89]$[70,73]
$O_2^-\cdot$ + $Fe^{3+} \rightarrow Fe^{2+} + O_2$	1.6e+6 ± 5.1e+5	$k[4]$[58,71,74,75]
H_2O_2 + Fe^{2+}-EDTA $\rightarrow Fe^{3+}$-EDTA + HO·	3.2e+5 ± 5e+5	$k[0]$[58,71,76]
HO· + LH $\rightarrow$ L· + H_2O	1e+9 ± 0	$k[3]$[11]
Chain Propagation		
L· + $O_2 \rightarrow$ LOO·	3.5e+8 ± 3.4e+8	$k[5]$[49,65,67]
LOO· + LH $\rightarrow$ LOOH + L·	39.8 ± 20.7	$k[6]$[49,68,77–79]
Termination		
L· + L· $\rightarrow$ L-L	5.8e+8 ± 5.1e+8	$k[60]$[49,65,67,80,81]
L· + LOO· $\rightarrow$ LOOL	5e+7 ± 0	$k[61]$[49,68]
LOO· + LOO· $\rightarrow$ LOOL + O_2	1.5e+7 ± 1.4e+7	$k[67]$[49,66–68,79,82]
Competing Reactions		
HO· + $Fe^{2+} \rightarrow Fe^{3+} + OH^-$	2.4e+9 ± 4e+9	$k[1]$[32,48,59]
HO· + $H_2O_2 \rightarrow H_2O + H^+ + O_2^-\cdot$	3.3e+7 ± 1.1e+7	$k[2]$[59,63]
HO· + GSH $\rightarrow$ GS· + H_2O	1.2e+10 ± 3.5e+9	$k[102]$[32,48]

One critical rate constant for which literature values varied was that for oxygen addition to lipid alkyl radicals, k[5], ranging from 10^7 to about 5×10^9, depending on the type of lipid radical, LH. In our standard model, we selected a conservative value for this rate constant for nonspecific lipids, 9×10^6, based on the work of Uri.[49] Since the lipid composition of various biological systems may vary greatly, we specifically explored results of simulations executed with rate constants for oxygen addition ranging from 10^6-10^{10}. The results are shown in Table 7 and indicate that large increases in the rate constant within the specified range, do not produce large increases in LOOH formation. The rate of oxygen addition is indeed quite fast, but lipid hydroperoxide formation is typically limited by generation of the lipid alkyl radical, L•.

Table 7. Effect of Changing the Rate Constant for Oxygen Addition to Various Lipids

Lipid	Rate Constant 1/(mol-s)	LOOH (μM)	L· (μM)	Chain Length
Unspecified (after Uri)	9e+6	351	205	1.71
Arachidonate	2e+8	438	205	2.13
Linoleate	3e+8	439	205	2.14
Oleate	1e+9	441	205	2.15
Methyl	5e+9	441	205	2.15

Prooxidant effects

Figure 3 illustrates the prooxidant effects of oxygen concentration upon overall lipid peroxidation in the undefended two-compartment model. The inset shows the final values for LOOH concentration at 10 min. LOOH formation depends on the presence of oxygen in a nonlinear fashion, half maximal responses occurring with about 30 μM oxygen. Air-saturated water at one atmosphere contains about 200 μM oxygen. Taking the corresponding conversion to partial pressure of 1 μM O_2 = 0.70 mmHg, one can appreciate that relatively low oxygen tensions in tissue are theoretically required to support lipid peroxidation, a finding in agreement with experimental data.[24]

Figure 4 shows the effect of increasing soluble iron concentrations in the presence and absence of antioxidant enzymes. Antioxidant enzymes alter both the maximal degree of lipid peroxidation and the shape of the iron-dependence curve. In the absence of SOD and CAT, lipid peroxidation is greatest, and maximal levels are produced with very low iron concentrations near 1 μM. Analysis of reaction fluxes revealed that under these conditions Fenton's reaction is limited by the rate of production of hydrogen peroxide, rather than by the availability of iron. When SOD alone is added, lipid peroxidation is quenched, and hydrogen peroxide is readily formed from superoxide. Under these conditions, hydrogen peroxide availability is no longer limiting; increasing iron levels engender increasing lipid peroxidation. The plateau of the iron-LOOH curve is shifted to the right, and the curve encompasses biologically relevant concentrations of iron. When both SOD and CAT are added, the effect is similar to that of SOD alone (Figure 4).
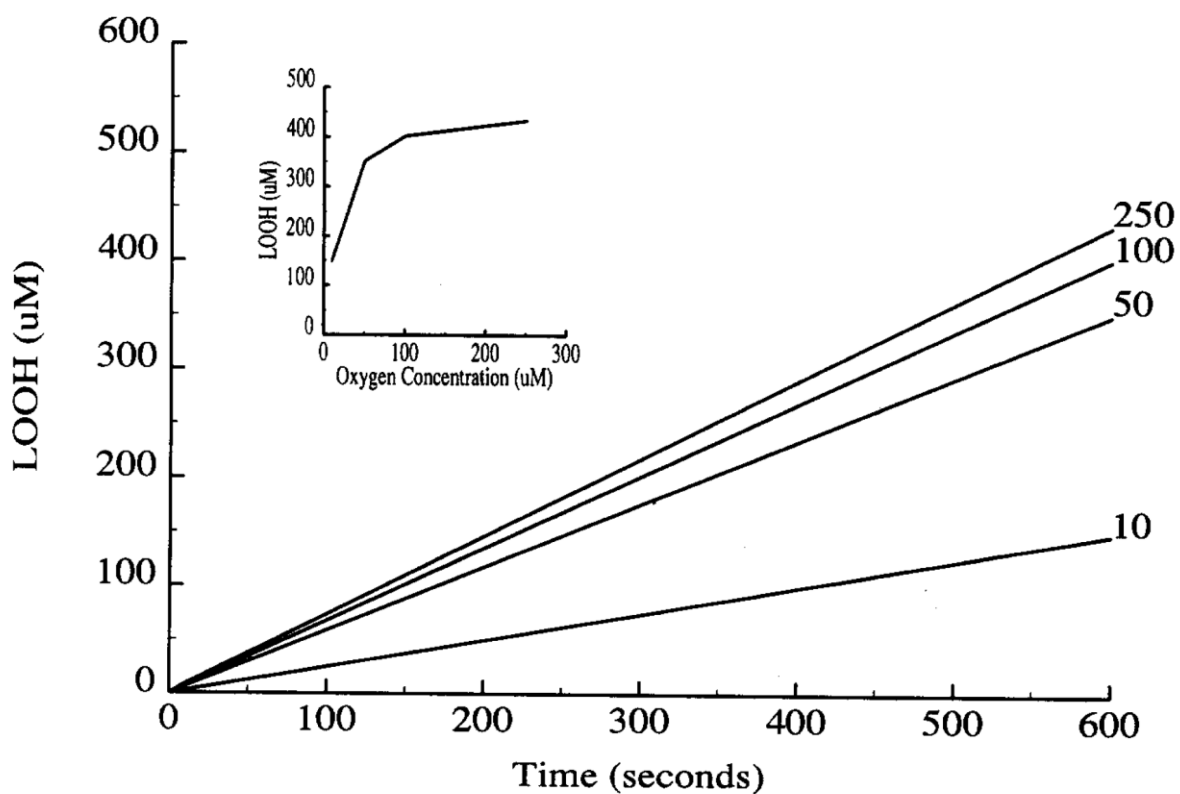
Fig. 3. Prooxidant effects of oxygen upon overall lipid peroxidation in the two compartment model. At a constant iron concentration (100 μM), the oxygen concentration was varied from 10 to 250 μM. The rate of LOOH formation is dependent upon oxygen concentration in a nonlinear fashion (inset). Inset shows final LOOH concentration at the end of a 10 min simulation as a function of oxygen concentration
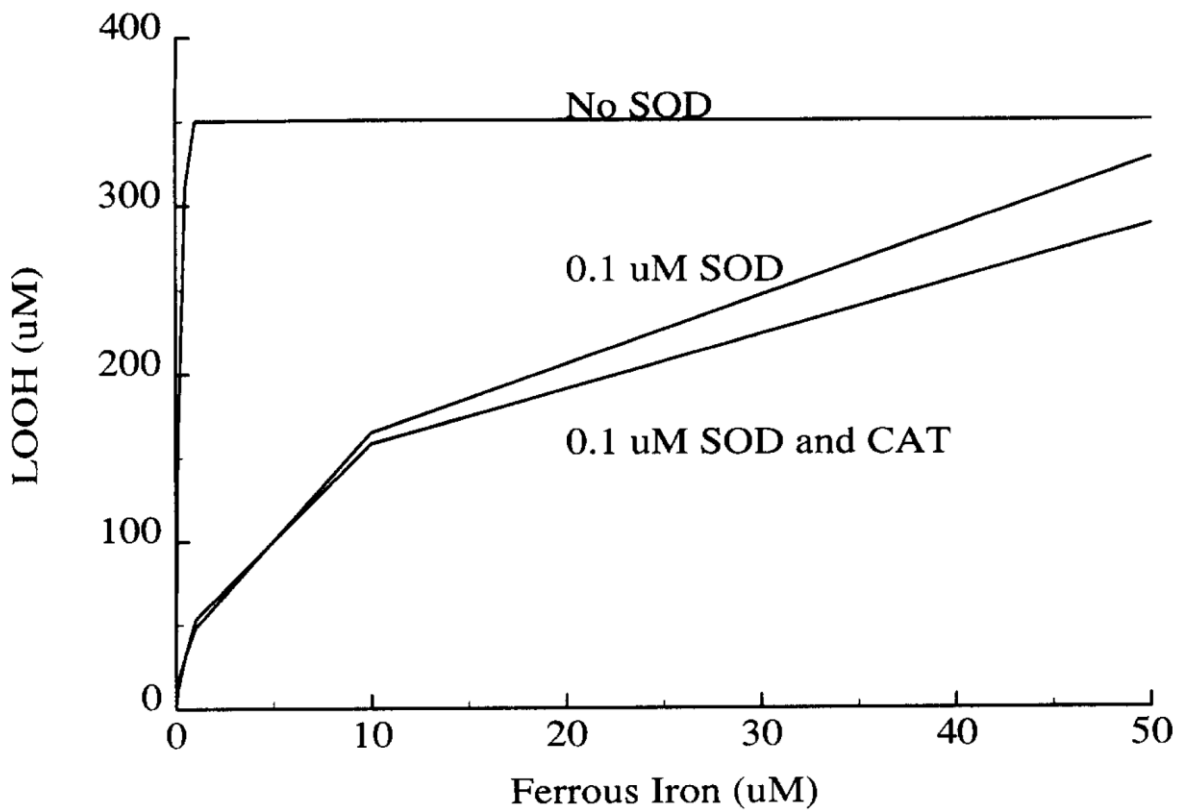
Fig. 4. Prooxidant effects of iron upon overall lipid peroxidation in the two compartment model, as influenced by antioxidant enzymes. At a constant oxygen concentration (50 µM), the iron concentration was varied from 0.01 to 50 µM. In the absence of antioxidant enzymes as little as 1 µM ferrous iron produces near maximal amounts of LOOH. In the presence of antioxidant enzymes the magnitude and shape of the curve describing iron-dependent production of LOOH are changed.

Iron and oxygen were highly effective species in our model in promoting lipid peroxidation, just as we have observed in the laboratory,[10, 24] but because of their nonlinear actions, higher concentrations tended to have small marginal effects. For the purpose of the present simulations, therefore, near-maximally effective levels of 100 µM Fe and 250 µM oxygen were used subsequently to provide a provocative test of antioxidant defense mechanisms.

Antioxidant defense mechanisms

Even in the presence of such near maximal oxidative stress, the production of lipid hydroperoxides was substantially reduced by the introduction of antioxidant defense mechanisms. In Fig. 5 the influence of increasing amounts of a vitamin E-like chain breaking antioxidant (AH) in the membrane compartment is demonstrated. Adding antioxidant in mean concentrations within the range reported for normal tissues (10 to 50 µM) suppresses the initial rate of lipid peroxidation until the antioxidant is consumed. During the antioxidant-induced induction period, measured between time zero and the break in slope of the curves in Fig. 5, little hydroperoxide is produced. Thereafter, production rises as if there were no antioxidant. The addition of antioxidant decreases the initial rate of lipid hydroperoxide formation (first 60 sec) from 0.74 to 0.54 µM/sec and then to 0.09 µM/sec with 0, 10, and 50 µM AH, respectively (inset). Higher, therapeutic concentrations of antioxidant had correspondingly greater effects, prolonging the duration of the induction period in proportion to the amount of antioxidant initially present. This effect is of chain-breaking antioxidants classically known for pure chemical systems.[11]

Addition of superoxide dismutase to the aqueous, cytosolic compartment of the model, as a sole antioxidant, induced a biphasic alteration in the computed amount of lipid peroxidation. Very small amounts of SOD alone slightly potentiated lipid peroxidation, but concentrations greater than 0.1 µM profoundly suppressed it (Fig. 6). The addition of cytosolic SOD + catalase, 1 to 10 µM in a 1:1 molar ratio, as roughly occurs in vivo,[50] substantially reduced lipid peroxidation to about one-tenth that in an undefended model (Fig. 7). SOD alone was nearly as effective as SOD + catalase, supporting the notion that SOD is the most important intracellular antioxidant enzyme.

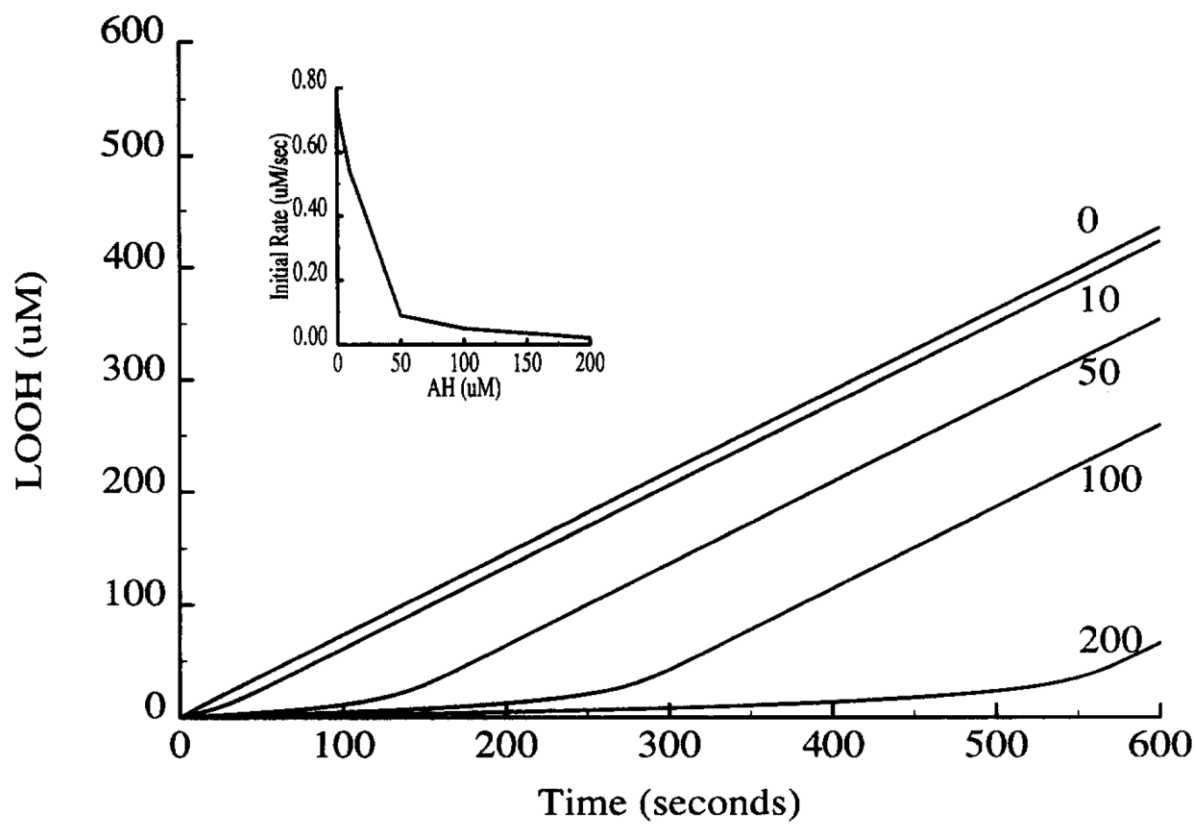Fig. 5. Influence of increasing amounts of a vitamin E-like chain breaking antioxidant (AH) in the membrane compartment. Initial conditions simulated near-maximal oxidant stress, with oxygen at 250 µM and ferrous iron at 100 µM. The presence of AH greatly decreases the initial rate of LOOH formation, as shown in the inset. After consumption of AH the rate of lipid peroxidation returns to the value observed in the absence of AH.
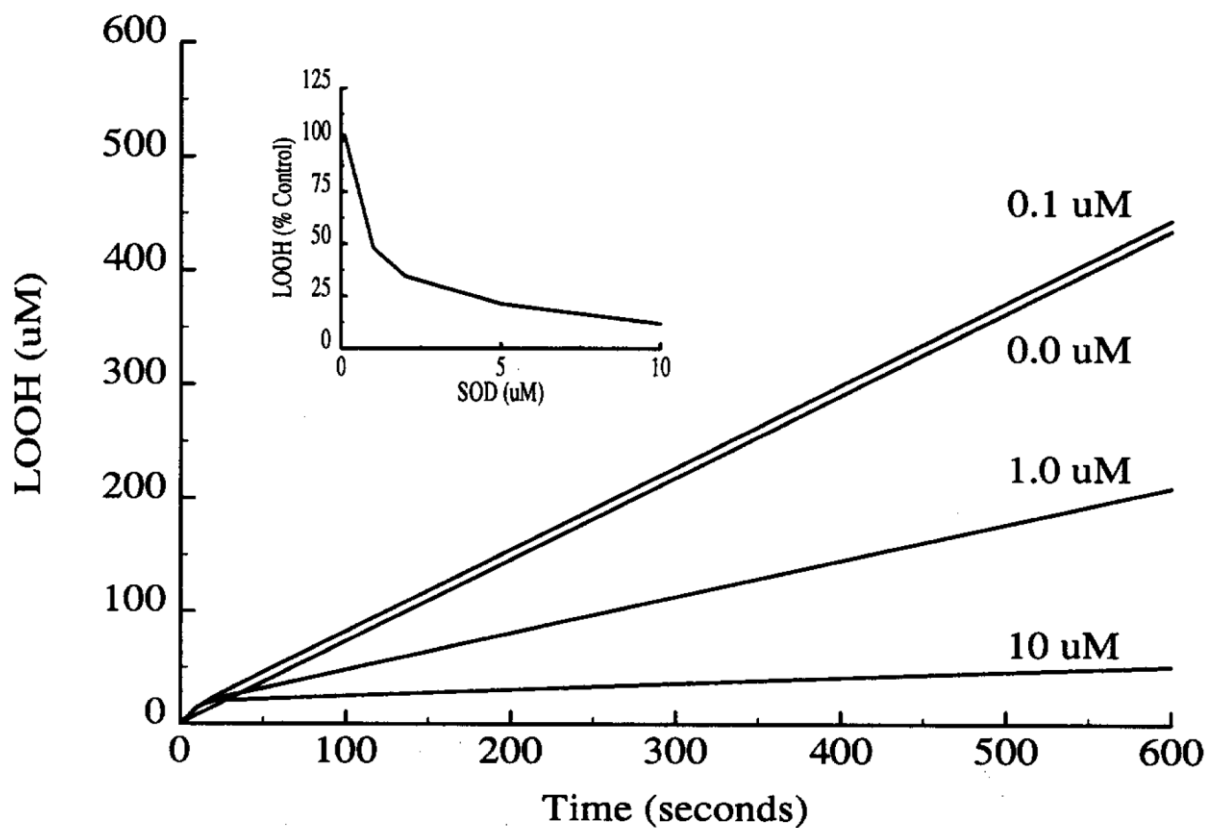
Fig. 6. Effects of SOD in simulated lipid peroxidation in the two compartment kinetic model. Increasing amounts of SOD from 0.1 to 10 μM progressively quench formation of LOOH. In the presence of ferrous iron initially, a small prooxidant effect is seen (Time 0--25 sec). Suppression of LOOH formation is dependent upon SOD concentration in a nonlinear fashion (inset).
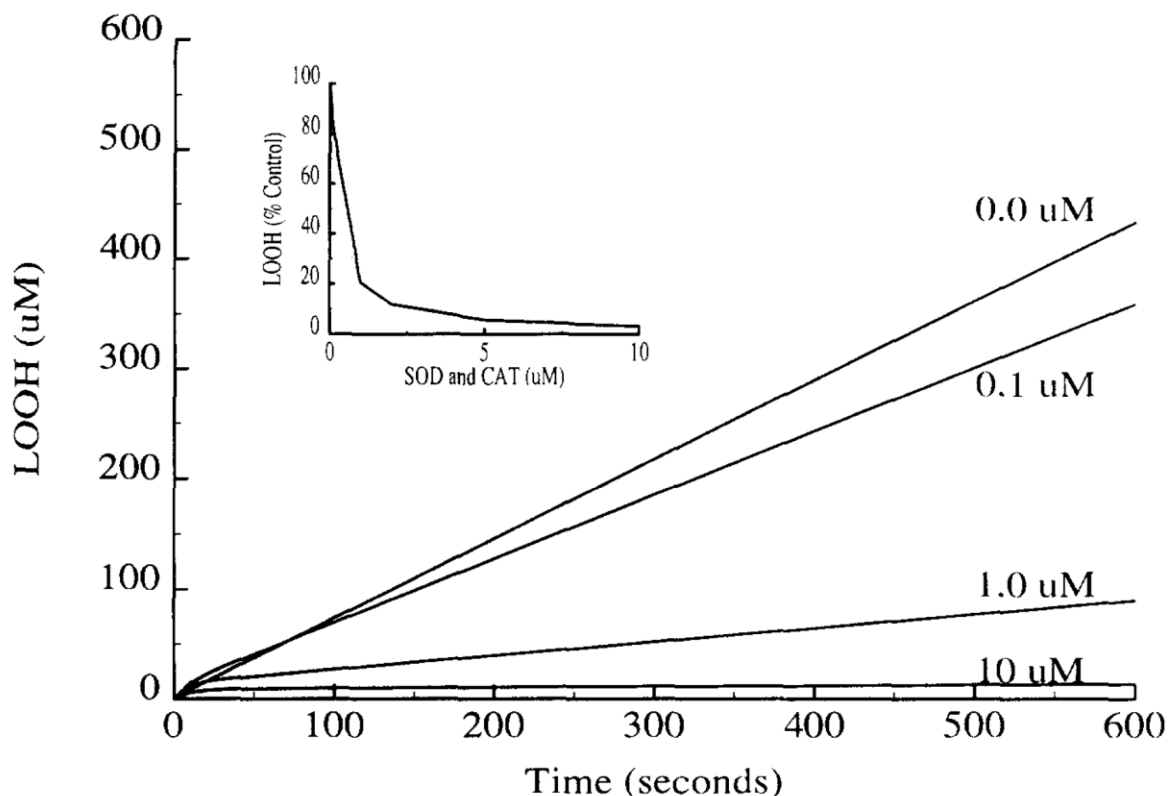
Fig. 7. Effects of equimolar SOD and catalase on simulated lipid peroxidation in the two compartment kinetic model. Increasing amounts of the dual antioxidant enzymes (0.1 to 10 µM) progressively quench formation of LOOH somewhat more than similar amounts of SOD alone. Suppression of LOOH formation is dependent upon SOD + CAT concentration in a nonlinear fashion (inset).

Absolute values of free radical concentrations

Table 8 presents absolute values of steady-state, instantaneous radical concentrations for typical defended and undefended tissue models during oxidative stress caused by 1 mM hypoxanthine and 0.15 µM xanthine oxidase. The values range from 10^{-15}-- 10^{-7} M, illustrating the extremely small absolute concentrations of reactive intermediate radicals that one would reasonably expect in a biological system. These small values help one appreciate why free radicals have been such elusive pathogens for so many years and why making direct measurements of specific radicals in vivo remains a formidable technical challenge.

Table 8. Absolute Values of Steady State Radical Concentrations

Radical Species	Steady State Concentration (M)	
	Undefended	Defended
HO·	$7e-09$	$7e-15$
L·	$2e-03$	$2e-09$
LOO·	$1e-04$	$1e-10$
R·	$1e-08$	$1e-14$
ROO·	$2e-07$	$2e-13$
A·	0	$1e-7$
GS·	$1e-04$	$1e-10$

DISCUSSION

Kinetic models, such as that herein described, can help to unify knowledge from many disciplines and to provide insight concerning mechanisms of free radical mediated tissue damage. The present simulations allowed us to explore quantitatively the specific chemical mechanisms by which "bursts" of oxygen-centered free radicals may alter membrane integrity through the mechanism of lipid peroxidation. Importantly, the simulations provided quantitative estimates suggesting that the various multifaceted antioxidant defenses against free radical-mediated lipid peroxidation can be extremely effective in defending cell membranes against oxidative stress derived from the metabolism of excess hypoxanthine by xanthine oxidase. The balance between oxidative stress and antioxidant defense mechanisms was revealed as a key to the understanding of the chemical mechanisms leading to lipid peroxidation.

In exploring factors that alter the oxidative stress/defense balance, computational models may provide helpful guides to productive research. Computer models of complex biological systems have become increasingly popular as research tools.[51] Such models can serve to sharpen intuition, to suggest interesting new experiments, and to explain or interpret results of previous ones. While they are by no means a substitute for experimental studies, computational models do require one to advance from qualitative theorizing--in the present case permitting quantitative predictions as to the numbers of free radicals of different types expected in the cytosolic and membrane compartments of cells in the face of oxidative stress. Most previously published theoretical discussions of free radical reactions in vivo have been qualitative in nature, with only implicit regard for rate constants of specific reactions. The development of a computer model, however, forces its creator to formulate concrete and specific hypotheses as to mechanisms and to state assumptions explicitly and quantitatively. The results of modeling provide quantitative tests of the proposed hypotheses and can be compared with analogous experimental results that are available.

The application of computer simulation to the study of free radicals in biology seems especially apt for two reasons. First, it is possible to focus a wealth of knowledge concerning the chemical kinetics of free radical reactions obtained from pulse radiolysis studies (references Table 2) upon the biological problem at hand. In this sense simulation models can provide focal points for integration and unification of much existing knowledge about free radical chemistry. A second

reason to apply computer models to the study of free radicals in biology relates to the exceedingly small instantaneous concentrations of free radicals in tissue, ranging from 10^{-15} to 10^{-7} M, which are so minute as to be extremely difficult to measure experimentally.

Direct measurement of free radicals in vivo, especially quantitative measurement, remains extremely difficult to perform. Indeed, the existence of pathologically significant numbers of free radicals in vivo remains an open question. Computer modeling offers one approach to addressing the question of whether numbers of reactive oxygen radicals, adequate to cause substantial cellular injury, could indeed be generated under plausible biological conditions. Computer modeling also offers a means of suggesting strategies to minimize free radical injury, when it is likely to occur.

Following this process, the authors have begun to develop insights into specific biological mechanisms. Hydroxyl radicals can be made by the superoxide-driven Fenton reaction in the presence of reactant concentrations likely to exist in vivo. In the absence of antioxidants, computed concentrations of lipid hydroperoxides equal or exceed those measured experimentally in some species after ischemia and reoxygenation.[52] However, antioxidants present in vivo have powerful quenching effects, such that the actual number of radical initiators depends very much upon the balance of prooxidant and antioxidant forces in the intracellular environment.

The compartmentalization of oxidizable lipids in membranes distinctly enhances the probability of chain propagation by making the effective concentrations of potential chain carriers and oxidizable lipids in the membrane much greater than their volume-averaged concentration. This compartmentalization of oxidizable lipids is key to understanding the apparent preferential damage to membranes caused by oxidative stress, and would seem to be a fundamental characteristic of cells and tissues.

Oxygen is required for lipid peroxidation, but because the rate constant for oxygen addition to L• is so great, only small concentrations of oxygen are required. This computational result is quite consistent with the proposition of Downey and coworkers[53] that reperfusion injury of heart muscle can occur "without reperfusion" in small myocardial infarcts. According to this concept, even though a coronary artery occlusion is never reopened, oxygen radical injury may develop in the border zones supplied by oxygen diffusion and "trickle" blood flow from adjacent normal muscle.

In addition to low levels of oxygen, only low concentrations of chelated, "free" iron are required for the initiation of lipid peroxidation. The results in Fig. 4, showing the iron dependence suggest that as little as 1 to 10 micromolar "free iron" is sufficient to support the superoxide driven Fenton reaction in simulated in vivo conditions. These results also, by implication, support the experimentally observed protective effects of strong iron chelators, like deferoxamine[54-56], which render soluble iron inactive in Fenton's reaction. Rapid chain propagation in membranes, however, is suppressed until there is consumption of membrane antioxidants, such as vitamin E. Just as is classically known in the study of bulk lipids[11], chain-breaking antioxidants are highly effective even in small concentrations, and protect against membrane lipid peroxidation until

they are consumed. Only after consumption of intra-membrane antioxidants, can membrane lipid peroxidation proceed at a vigorous rate by chain propagation.[11, 57]

In general, membrane lipid peroxidation requires breakdown in the normal balance between oxidative stress and the multilayered antioxidant defenses of living tissue. The present modeling studies suggest that only when defense mechanisms are eroded through underlying disease or prolonged oxidative stresses does rapid membrane lipid peroxidation occur.

REFERENCES

1. Slater, T. E *Free radical mechanisms in tissue injury.* London: Pion Limited; 1972.

2. Bulkley, G. B. The role of oxygen free radicals in human disease processes. *Surgery* 94:407-411; 1983.

3. Halliwell, B.; Gutteridge, J. M. C. Oxygen toxicity, oxygen radicals, transition metals and disease. *Biochem J* 219:1-14; 1984.

4. Halliwell, B.; Gutteridge, J. M. C. *Free radicals in biology and medicine.* Oxford: Oxford University Press; 1987:206-234.

5. Aust, S. D.; Morehouse, L. A.; Thomas, C. E. Hypothesis paper--role of metals in oxygen radical reactions. *Free Radical Biol Med* 1:3-25; 1985.

6. Babbs, C. E Reperfusion injury of postischemic tissues. *Ann of Emerg Med* 17:1148-1157; 1988.

7. Grootveld, M.; Halliwell, B. Aromatic hydroxylation as a potential measure of hydroxyl radical formation in vivo. *Biochem* J 237:499-504; 1986.

8. Halliwell, B.; Grootveld, M.; Gutteddge, J. M. C. Methods for the measurement of hydroxyl radicals in biochemical systems: deoxyribose degradation and aromatic hydroxylation. *Methods Biochem Anal* 33:59-90; 1987.

9. Babbs, C. E; Gale, M. J. Methane sulfinic acid production from DMSO as an indicator of hydroxyl radical production in vivo. In *Free radicals: methodology and concepts.* Rice-Evans, C.; Halliwell, B., eds. London: Richelieu Press; 1988:91-121.

10. Babbs, C. E; Griffin, D. W. Scatchard analysis of methane sulfinic acid production from dimethyl sulfoxide: a method to quantify hydroxyl radical formation in physiologic systems. *Free Radical Biol Med* 6:493-503; 1989.

11. Walling, C. *Free radicals in solution.* New York: John Wiley & Sons, Inc.; 1957.

12. Gimblett, E G. R. *Introduction to the kinetics of chemical chain reactions.* New York: McGraw-Hill; 1970.

13. Emanuel, N. M. The kinetic features of the chain mechanism of liquid-phase oxidation processes. In *Problems in chemical kinetics.* Emanuel, N., ed. Moscow: MIR Publishers; 1981.

14. Yang, C. H. On the explosion glow and oscillation phenomena in the oxidation of carbon monoxide. *Combustion and Flame* 23:97-108; 1974.

15. Levitsky, A. A.; Polyak, S. S.; Shtern, V. Y. Mechanism of propane oxidation-mathematical modeling, *Int J Chem Kinetics* 16:1275-1285; 1984.

16. Dodge, M. C.; Hecht, T. A. Rate constant measurements needed to improve a general kinetic mechanism for photochemical smog. *Int J Chem Kinetics* 7:155-163; 1975.

17. Hecht, T. A.; Seinfeld, J. H. Development and validation of a generalized mechanism for photochemical smog. *Environmental Science & Technology* 6, no. 1:47-57; January 1972.

18. Tappel, A. L.; Tappel, A. A.; Fraga, C. G. Application of simulation modeling to lipid peroxidation processes. *Free Radical Biol Med* 7:361-368; 1989.

19. McCord, J. M. Oxygen-derived free radicals in postischemic tissue injury. *New England Journal of Medicine* 312:159-163; 1985.

20. Bulkley, G. B. Free radical-mediated reperfusion injury: a selective review. *Br J Cancer (Suppl VIII)* 55:66-73; 1987.

21. Fischer, J. H.; Kulus, D.; Hansen-Schmidt, I.; Isselhard, W. Adenine nucleotide levels of canine kidneys during hypothermic perfusion. *Eur Surg Res* 13:178-188; 1981.

22. Kleihues, P.; Kobayashi, K.; Hossmann, K. A. Purine nucleotide metabolism in the cat brain after one hour of complete ischemia. *J Neurochem* 23:417-425; 1974.

23. Aust, S. D.; Svingen, B. A. The role of iron in enzymatic lipid peroxidation. In *Free radicals in biology,* vol. V. New York: Academic Press; 1982:1-28.

24. Salaris, S. C.; Babbs, C. F. The effect of oxygen concentration on the formation of malondialdehyde-like material in a model of tissue ischemia and reoxygenation. *Free Radical Biol Med.* 7:603-609; 1989.

25. Meerson, F. Z.; Kagan, V. E.; Kozlov, Y. P.; Belkina, L. M.; Arkhipenko, Y. V. The role of lipid peroxidation in pathogenesis of ischemic damage and the antioxidant protection of the heart. *Basic Res Cardiol* 77:465-485; 1982.

26. Aust, S. D.; Thomas, C. E.; Morehouse, L. A.; Saito, M.; Bucher, J. R. Active oxygen and toxicity. *Adv Exper Medicine & Biol* 197:513-526; 1986.

27. Fraga, C. G.; Leibovitz, B. E.; Tappel, A. L. Lipid peroxidation measured as thiobarbituric acid-reactive substances in tissue slices: characterization and comparison with homogenates and microsomes. *Free Rad Biol Med* 4:155-161; 1988.

28. Sano, M.; Motchnik, P. A.; Tappel, A. L. Halogenated hydrocarbons and hydroperoxide-induced lipid peroxidation in rat tissue slices. *Free Radical Biol Med* 2:41-48; 1986.

29. Benedetti, A.; Comporti, M.; Esterbauer, H. Identification of 4-hydroxynonenal as a cytotoxic product originating from the peroxidation of liver microsomal lipids. *Biochimica et Biophysica Acta* 620:281-296; 1980.

30. Krause, G. S.; White, B. C.; Aust, S. D.; Nayini, N. B.; Kumar, K. Brain cell death following ischemia and reperfusion: a proposed biochemical sequence. *Critical Care Medicine* 16:714-726; 1988.

31. Carnahan, B.; Luther, H. A.; Wilkes, J. O. *Applied numerical methods.* New York: John Wiley & Sons; 1969.

32. Spinks, J. W. T.; Woods, R. J. *An introduction to radiation chemistry, second ed.* New York: Wiley-Interscience; 1976.

33. Walsh, C. *Enzymatic reaction mechanisms.* San Francisco: W. H. Freeman & Co.; 1979.

34. Bielski, B. H. J.; Cabelli, D. E.; Arudi, R. L.; Ross, A. B. Reactivity of HO_2/O_2*-radicals in aqueous solution. *J Phys Chem Ref Data* 14:1041-1100; 1985.

35. Schonbaum, G. R.; Chance, B. Catalase. In P. D. Boyer, ed. *The enzymes,* vol. XIII, Part C. New York: Academic Press; 1976:363-399.

36. Spector, W. S., ed. *Handbook of biological data.* Philadelphia: W. B. Saunders Company; 1956:70-77.

37. Jennings, R. B.; Schaper, J.; Hill, M. L.; Steenbergen, C.; Reimer, K. A. Effect of reperfusion late in the phase of reversible ischemic injury. *Circulation Research* 56:262-278; 1985.

38. Buhl, M. R. Oxypurine excretion during kidney preservation: an indicator of ischemic damage. *Scand J Clin Lab Invest* 36:169-174; 1976.

39. Ratych, R. E.; Bulkley, G. B. Free-radical-mediated postischemic reperfusion injury in the kidney. *J Free Radical Biol Med* 2:311-319; 1986.

40. Battelli, M. G.; Della-Corte, E.; Stirpe, F. Xanthine oxidase type D (dehydrogenase) in the intestine and other organs of the rat. *Biochem J* 126:747-749; 1974.

41. Tien, M.; Svingen, B. A.; Aust, S. D. Superoxide-dependent lipid peroxidation. *Federation Proc* 40:179-182; 1981.

42. Holt, S.; Gunderson, M.; Joyce, K.; Nayini, N. R.; Eyster, G. F.; Garitano, A. M.; Zonia, C.; Krause, G. S.; Aust, S. D.; White, B. C. Myocardial tissue iron delocalization and evidence for lipid peroxidation after two hours of ischemia. *Annals of Emergency Medicine* 15:1155-1159; 1986.

43. Krause, G. S.; Joyce, K. M.; Nayini, N. R.; Zonia, C. L.; Garritano, A. M.; Hoehner, T. J.; Evans, A. T.; Indrieri, R. J.; Huang, R. R.; Aust, S. D.; White, B. C. Cardiac arrest and resuscitation: brain iron delocalization during reperfusion. *Ann Emerg Med* 14:1037-1043; 1985.

44. Aust, S. D. Sources of iron for lipid peroxidation in biological systems. In *Oxygen radicals and tissue injury (proceedings of a Brook Lodge symposium).* Halliwell, B., ed. Bethesda, MD: Federation of American Societies for Experimental Biology (FASEB); 1987:27-33.

45. Smith, J. B.; Cusumano, J. C.; Babbs, C. F. Quantitative effects of iron chelators on hydroxyl radical production by the superoxide-driven Fenton reaction. *Free Radical Research Communications* 8:101-106; 1990.

46. National Research Council U.S. International critical tables of numerical data, physics, chemistry, and technology. New York: International Council of Scientific Publishing for National Research Council, McGraw-Hill; 1926.

47. Babior, B. M.; Curnutte, J. T.; Okamura, N. The respiratory burst oxidase of the human neutrophil. In *Oxygen radicals and tissue injury (proceedings of a Brook Lodge symposium).* Halliwell, B., ed. Bethesda, MD: Federation of American Societies for Experimental Biology (FASEB); 1987.

48. Buxton, G. V.; Greenstock, C. L.; Helman, W. P.; Ross, A. B. *Critical review of rate constants for reactions of hydrated electrons, hydrogen atoms and hydroxyl radicals in aqueous solution.* Notre Dame, IN: Radiation Chemistry Data Center, Radiation Laboratory University of Notre Dame; June, 1986.

49. Uri, N. Physio-chemical aspects of autoxidation. In *Autoxidation and antioxidants.* Lundberg, W. O., ed. New York: Wiley-Interscience; 1961:55-106.

50. Fridovich, I. Superoxide radical: an endogenous toxicant. *Ann Rev Pharmacol Toxicol* 23:239-257; 1983.

51. Iyengar, S. S. *Computer modeling of complex biological systems.* Boca Raton, FL: CRC Press; 1984.

52. Salaris, S. C.; Babbs, C. F. A rapid, widely applicable screen for drugs that suppress free radical formation in ischemia/reperfusion. *Journal of Pharmacological Methods* 20:335-345; 1988.

53. Akizuki, S.; Yoshida, S.; Chambers, D. E.; Eddy, L. J.; Parmley, L. F.; Yellon, D. M.; Downey, J. M. Infarct size limitation by the xanthine oxidase inhibitor, allopurinol, in closed-chest dogs with small infarcts. *Cardiovascular Research* 19:686-692; 1985.

54. Gutteridge, J. M. C.; Richmond, R.; Halliwell, B. Inhibition of the iron-catalyzed formation of hydroxyl radicals from superoxide and lipid peroxidation by desferrioxamine. *Biochem J* 184:469-472; 1979.

55. Kompala, S. D.; Babbs, C.F.; Blaho, K. E. Effect of deferoxamine on late deaths following cardiopulmonary resuscitation in rats. *Annals Emerg Med* 15:405-407; 1986.

56. Ambrosio, G.; Zweier, J. L.; Jacobus, W. E.; Weisfeldt, M. L.; Flaherty, J. T. Improvement of postischemic myocardial function and metabolism induced by administration of deferoxamine at the time of reflow: the role of iron in the pathogenesis of reperfusion injury. *Circulation* 75:906-915; October 1987.

57. Paller, M. S. Renal work, glutathione and susceptibility to free radical-mediated injury. *Kidney International* 33:843-849; 1988.

58. Ilan, Y. A.; Czapski, G. The reaction of superoxide radical with iron complexes of EDTA studied by pulse radiolysis. *Biochim Biophys Acta* 498:386-394; 1977.

59. Walling, C. Fenton's reagent revisited. *Accounts of Chemical Research* 8:125-131; 1975.

60. Reich, L.; Stivala, S. S. *Autoxidation of hydrocarbons and polylegins--kinetics and mechanisms.* New York: Marcel Dekker, Inc.; 1969.

61. Barman, T. E. In *Enzyme handbook, vol. I.* New York: Springer- Verlag; 1969:232-233.

62. Bielski, B. H. J.; Allen, A. O. Mechanism of the disproportionation of superoxide radicals. *J Physical Chemistry* 81:1048-1050; 1977.

63. Dorfman, L. M.; Adams, G. E. Reactivity of the hydroxyl radical in aqueous solutions. National Standard Reference Data Series 46 (NSRDS-NBS46), U.S. National Bureau of Standards. Washington, DC: U.S. Government Printing Office; 1973.

64. Neta, P.; Ross, A. B. Representative rate constants for radical reactions of biologically important molecules. In *Chemical kinetics of small organic radicals.* Boca Raton: CRC Press; 1988:187-212.

65. Ross, A. B.; Neta, P. Rate constants for reactions of aliphatic carbon-centered radicals in aqueous solution. National Standard Reference Data Series 70 (NSRDS-NBS70), U.S. National Bureau of Standards. Washington, DC: U.S. Government Printing Office; 1982:1-97.

66. Frimer, A. A. Organic reactions involving the superoxide anion. In Patai, S., ed. *The chemistry of functional groups peroxides.* John Wiley & Sons Ltd; 1983:429-461.

67. Chambers, D. E.; Parks, D.. A.; Patterson, G.; Roy, R.; McCord, J. M.; Yoshida, S.; Parmley, L. F.; Downey, J. M. Xanthine oxidase as a source of free radical damage in myocardial ischemia. *J Mol Cell Cardiol* 17:145-152; 1985.

68. Aaes-Jorgensen. Autoxidation of fatty compounds in living tissue biological antioxidants. In Lundberg, E. O., ed., *Autoxidation and antioxidants vol. H.* Wiley-Interscience; New York: 1962:1045-1094.

69. Rigo, A.; Viglino, P.; Rotitio, G. Kinetic study of O_2-dismutation by bovine superoxide dismutase. Evidence for saturation of the catalytic sites by O_2. *Biochem Biophys Comm Res* 63:1013-1018; 1975.

70. Massey, V.; Brumby, P. E.; Komai, H.; Palmer, G. Studies on milk xanthine oxidase--some spectral & kinetic properties. J *Biol Chem* 224:1682-1691; 1969.

71. Bull, C.; McClune, G. J.; Fee, J. A. The mechanism of Fe- EDTA catalyzed superoxide dismutation. *J Am Chem Soc* 105:5290-5300; 1983.

72. Howard, J. A.; Scaiano, J. C. Landolt-Bornstein Volume 13C. Fischer, H., ed. New York: Springer-Verlag; 1984.

73. Bray, R. C. Molybdenum iron-sulfur flavin hydroxylases and related enzymes. In *The enzymes,* vol. XII. Boyer, P. D., ed. New York: Academic Press; 1975.

74. Butler, J.; Halliwell, B. Reaction of iron-EDTA chelates with the superoxide radical. *Arch Biochem Biophys* 218:174-178; 1982.

75. Bull, C.; Fee, J. A.; O'Neill, P.; Fielden, E. M. Iron-ethylenediaminetetraacetic acid (EDTA)-catalyzed superoxide dismutation revisited: an explanation of why the dismutase activity of Fe-EDTA cannot be detected in the cytochrome c/xanthine oxidase assay system. *Arch Biochem Biophys* 215:551-555; 1982.

76. Borggaard, O. K.; Farver, O.; Anderson, V. Polarographic study of the rate of oxidation of iron(II) chelates by hydrogen peroxide. *Acta Chem Scand* 25:3541-3543; 1971.

77. Semenov, N. N. *Some problems of chemical kinetics and reactivity volume one.* New York: Pergamon Press; 1958.

78. Denisov, E. T.; Mitskevich, N. I.; Agabekov, V. E. *Liquid phase oxidation of oxygen-containing compounds.* New York: Consultants Bureau; 1977.

79. Neta, P.; Huie, R. E.; Ross, A. B. Rate constants for reactions of peroxyl radicals in fluid solutions. *J Phys Chem Ref Data* manuscript submitted for publication.

80. Stevens, G. C.; Clarke, R. M.; Hart, E. J. Radiolysis of aqueous methane solutions. *J Phys Chem* 76:3863-3867; 1972.

81. Swallow, A. J. *Radiation chemistry, an introduction.* New York: Halstead Press; 1973.

82. Semenov, N. N. *Some problems of chemical kinetics and reactivity volume two.* New York: Pergamon Press; 1959.

APPENDIX

Consider a biological system containing two compartments, nominally an aqueous compartment, 1, and a lipid compartment, 2. Let the following variables be defined, as in Table 3.

V_1	aqueous volume
V_2	lipid volume
V_T	total volume
$r = \dfrac{V_1 + V_2}{V_2}$	compartment volume ratio (>1)
$q_A = \dfrac{[A]_2}{[A]_1}$	lipid/water partition coefficient for reactant, A
$q_B = \dfrac{[B]_2}{[B]_1}$	lipid/water partition coefficient for reactant, B
c_1	reactant concentration in compartment 1
c_2	reactant concentration in compartment 2
$\bar{c}$	volume averaged, mean concentration in both compartments

Combining the defining expressions, the concentrations of reactants in the individual compartments 1 and 2 are easily shown to be related to the mean, volume averaged reactant concentrations as follows:

$$c_1 = \frac{r}{q + r - 1}\,\bar{c} = \theta_1\bar{c} \text{ and } c_2 = \frac{qr}{q + r - 1}\,\bar{c} = \theta_2\bar{c}. \quad (1)$$

A generalized analysis of reactions taking place in either or both phases is as follows. For the reaction

$$A + B \xrightarrow{k} \text{products} \qquad (2)$$

the change in mean concentrations of A and B (denoted [A] and [B]) due to the reaction in compartment 1 (aqueous) only are

$$\frac{-d[A]_1}{dt} = \frac{-d[B]_1}{dt} = \frac{kc_{1A}c_{1B}V_1}{V_1 + V_2} = k\theta_{1A}[A]\theta_{1B}[B](1 - 1/r). \qquad (3)$$

Similarly, the changes in mean concentration of reactants A and B due to the reaction in (lipid) compartment 2 only are

$$\frac{-d[A]_2}{dt} = \frac{-d[B]_2}{dt} = \frac{kc_{2A}c_{2B}V_2}{V_1 + V_2} = kq_A\theta_{1A}[A]q_A\theta_{1B}[B](1/r). \qquad (4)$$

Combining expressions (3) and (4) the change in mean concentration due to reactions in **both** compartments,

$$\frac{-d[A]}{dt} = \frac{-d[A]_1}{dt} + \frac{-d[B]_1}{dt}$$

$$= (\,(1-1/r) + q_A q_B(1/r)\,)\theta_{1A}\theta_{1B}k[A][B]. \qquad (5)$$

Substituting

$$\theta_{1A} = r(q_A + r - 1) \text{ and } \theta_{1B} = r/(q_B + r - 1)$$

and rearranging, we find the mean, volume averaged, reaction rate for the two phase system is

$$\frac{-d[A]}{dt} = \frac{(q_A q_B + r - 1)r}{(q_A + r - 1)(q_B + r - 1)} k[A][B] = k_{eq}[A][B], \qquad (6)$$

as presented in the text. Thus, the mean, volume averaged rate of reaction in the two compartment model is directly proportional to the reaction rate, k[A][B], that would have occurred if the reactants had been uniformly distributed in solution in a one-compartment model at their mean concentrations.